Green Synthesis of Tin Oxide Nanoparticles using *Psidium guajava* Leaves Extract and its Applications in Antibacterial and Antioxidant Activities

Tirtha Raj Binadi*, Paramatma Mishra, Bhoj Raj Poudel, Surendra K Gautam*

Department of Chemistry, Tri-Chandra Campus, Tribhuvan University, Nepal

*Corresponding E-mail: binaditirtharaj@gmail.com; surendra.gautam@trc.tu.edu.np

Abstract

In this study, tin oxide (SnO_2) nanoparticles was synthesized via green synthetic route using *Psidium guajava* (Guava) leaf extract as reducing, capping and stabilizing agents. The synthesized SnO_2 NPs were characterized by X-ray diffraction (XRD), Fourier transform infrared spectroscopy (FTIR) and UV-visible spectroscopy. The XRD analysis revealed that synthesized SnO_2 nanoparticles have tetragonal rutile structure, and the particle size was found to be 19.5 nm estimated by using Debye-Scherer's equation. In addition, the average particle size calculated by using Williamson-Hall plot method was found to be 21.5 nm. The FTIR spectra reveals hydroxyl, alkyl, alkane, amide and hydroxyl tin group as a functional group. UV-Visible absorption spectra were found to be 270 nm, and its corresponding band gap energy was found to be 3.88 eV. Moreover, the antimicrobial activities of different concentrations of SnO_2 NPs using *Psidium guajava* leaf extract were also tested. Accordingly, the result showed that the highest zone of inhibitions was measured for SnO_2 NPs using 30mg/mL solution concentration and observed to be 18mm, 21mm and 20mm for *S. aereus, P. aeruginosa* and *K. pneumoniae* respectively. As synthesized SnO_2 NPs also showed significant antioxidant efficacy against 2,2-diphenyl-1-picrylhydrazyl radical.

Keywords: SnO_2-NPs; Green synthesis; Band gap; Antibacterial; Antioxidant

Introduction

In recent years, nanotechnology has received a tremendous boost generating a multitude of scientific ideas that compete with the everyday challenges of growing technology. Nanomaterials have attracted diverse scientific and technological interest due to their countless applications and specific properties [1,2]. Materials which have at least one dimension (length or width or height) in the range of 1-100 nm are called nanomaterials. Nanoparticles have high applications potentials due to their unique mechanical, thermal, electrical, magnetic, catalytic and optical properties [3,4]. SnO_2 is one of the most important materials due to its high degree of transparency in the visible spectrum, strong physical and chemical interaction with adsorbed species, low operating temperature and strong thermal stability. SnO_2 is a n-type semiconductor with a wide direct band gap (3.6 eV at 300 K) [5]. It is widely used in optoelectronic devices, electrodes for lithium-ion batteries, solar cells, transistors and gas sensors to detect the combustible gases such as H_2S, CO, liquid petroleum, NO, NO_2 and C_2H_5OH [5,6]. Tin oxide nanoparticles are suitable for gas sensing applications due to high surface to volume ratio, compared to bulk tin oxide, which results in increased sensitivity and adsorption.

Tin oxide nanoparticles have been prepared by physical and chemical methods [7,8]. SnO_2 has a key advantage over other materials such as TiO_2, since it offers high electron mobility (100-200 cm^2 V^{-1} s^{-1}) leading to faster photo generated electron transport [9]. There are many

methods for preparation of SnO_2 nanoparticles (NPs) [10, 11] but bio-based green synthesis approach has gained considerable interest [12, 13]. Bio-based green synthesis methods using plant extracts are considered eco-friendly, safe and cheap but, only few reports are available throughout the literature regarding green synthesis of SnO_2 NPs [14, 15].

Here in this paper, we have synthesized SnO_2 NPs using guava (*Psidium guajava*) leaf extracts by a simple and economical synthesis method [16-18]. Guava leaf extracts have found to contain phenolic compounds, flavonoids, sesquiterpene alcohols and triterpenoid acids which possess antioxidant, antimicrobial as well as antitumor properties [19, 20]. The structural characterization of synthesized NPs was extensively examined using X-ray diffraction (XRD), Fourier transform infrared spectroscopy (FTIR) and UV-Visible spectroscopy technique [21, 22]. Therefore, this work aimed to explore the application of *Psidium guajava* leaves extract as a capping and reducing agent for the synthesis of SnO_2 NPs and evaluate the antibacterial activities of the synthesized SnO_2 NPs against selected pathogenic using the agar disc diffusion method. In addition, this work opens a door for further investigation on many medicinal plants for nanomaterials synthesis which could be used for various applications.

Materials and Methods
Study Area

The leaves of *P. guajava* (Guava) were collected from the Kathmandu district. Laboratory grade chemicals such as $SnCl_2.2H_2O$, doubled distilled water, DPPH (2,2-diphenyl-1-picrylhydrazyl), methanol agar plate and DMSO (Dimethyl sulfoxide) were marketed by local supplier of Kathmandu and other chemicals were used throughout the experiment.

Methods

About 50 g of leaves was weighed and washed thoroughly in distilled water for 5 min. Then the leaves were subjected to dry at room temperature. Then, the dried leaves were cut into fine pieces and was boiled in 500 mL conical flask with 200 mL of distilled water at 80-90℃ for 30 min and allowed to cool down for a day and was filtered using Whattmann's filter paper No.41. Solution obtained from filtration process was used as guava leaf extract and was stored in the refrigerator at 4℃ until needed.

Synthesis of SnO_2 nanoparticles

About 11.28 g of $SnCl_2.2H_2O$ was weighed exactly and dissolved in 100 mL of double distilled water to prepare 0.5 M tin chloride solution ($SnCl_2.2H_2O$). Then it was allowed to stir for 24 hours for complete dissolution and finally the 100 mL of 0.5 M tin chloride solution was prepared and was ready to use for the synthesis of SnO_2 nanoparticles. 70 mL of $SnCl_2.2H_2O$ solution was taken from the stock solution. To this stock solution, 30 mL of leaf extract obtained from *Psidium guajava* was added via burette. After appearing light brown colored precipitate of tin hydroxide $Sn(OH)_2$, it was allowed to boil at 70-80℃ for 30 min, and the cooled down for 24 hours for nucleation. Then the ppt was allowed to settle down and filtered using Whatmann's filter paper No.41. The filtered ppt was washed with distilled water for 3-4 times and allowed to dry at room temperature and was kept at oven at 80℃ for 24 hours. After this, it was crushed finely into powder with mortar in crucible and was calcinated at 400℃ for 3 hours. Finally, SnO_2 nanoparticles were obtained.

Characterization methods

XRD analysis of sample were carried out by using CuKα radiation of wavelength λ = 0.15406 nm on a Rigaku 18kW rotating anode-based powder diffractometer working in Bragg-Brentano geometry and fitted with the curved crystal graphite monochromator in the diffracted beam. Collection of data was done in

continuous scan mode in the 2theta range of 10-90 degree at a scan rate of two degree per minute and a step interval of 0.02 degrees [23]. The X-ray generator was operated at 40kV voltage and 150 mA tube current, which was found to be adequate for characterizing the nanoparticles. The average particle size was determined from full width at half maximum (FWHM) of a peak form XRD spectra after removing instrumental broadening using Debye-Scherrer`s equation [24],

$$D = 0.94\lambda/\beta Cos\theta \qquad (1)$$

Where,

D= Average diameter of nanoparticles

λ= Wavelength of CuKα radiation (0.15406 nm)

β= Full width at half maximum (FWHM)

θ= Angle of diffraction

Fourier-transform infrared (FTIR) spectroscopy was used in the identification of the infrared spectra of synthesized NPs using an IR-Tracer-100 Spectrometer in the wavenumber range of 500-4000 cm^{-1} [25].

Ultraviolet-Visible (UV-Vis) Spectroscopy was performed using Chemiton UV-Visible spectrophotometer for the analysis of the optical properties of synthesized NPs. The well dispersed solution of SnO$_2$ NPs was used, and its absorbance was measured in the wavelength region of 150-500 nm [26].

Antibacterial Activity

For the antibacterial test, three bacterial species*: Klebseilla pneumoniae, Pseudomonas aeruginosa and Staphylococcus aureus* were taken. 100μL culture broths was spread into nutrient-agar plate (2.5 g/L nutrient media and 2.5 g/L agar) and incubated at 30℃ for 15 minutes. The agar plate is levelled with the help of marker then 10 μL of tin oxide nanoparticles solution synthesized by using *Psidium guajava* was uploaded separately on three parts of each of agar plate carefully with different concentration 10mg/mL, 20mg/mL and 30mg/mL respectively and incubated overnight at 37℃. After 24 hours the antibacterial and of the tin oxide nanoparticles was observed. Here, kanamycin was used as standard or positive control and DMSO was used as negative control. The concentration of kanamycin was 5mg/mL and 5 µL was uploaded in each agar plate [25].

Antioxidant activity

For the determination of antioxidant property 2, 2-diphenyl-1-picrylhydrazyl (DPPH) method was used. For this 0.77 mg of DPPH was dissolved in 100 mL of 99% methanol and stored in dark at -5℃. The free radical scavenging activity of tin oxide nanoparticles was determined using the stable radical DPPH. 1 mL of different concentrations (10, 20, 30, 40, 50, 75 and 100 mg/mL) of tin oxide nanoparticles was mixed with 1 mL of freshly prepared DPPH which was prepared by dissolving 0.77 mg of DPPH in 100 mL of methanol. Then the solution was incubated at room temperature in the dark for 30 min. The absorbance was recorded at 517 nm using UV-visible spectrophotometer. DPPH was used as a control and methanol was used as a blank solution. The free radical scavenging activity was expressed as the percentage of inhibition which was determined using the following formula.

% of scavenging = P_c-P_s/P_c×100

Where, P_c is the absorbance of control (methanol) and P_s is the absorption of tin oxide nanoparticles [27].

Results and Discussion
X-ray Diffraction (XRD) Analysis

X-ray diffraction is a non-destructive technique for characterizing crystalline materials or materials with some crystalline domains in them. XRD is unique in providing a wide variety of information on crystal structure, crystalline phases, preferred crystal orientation

and other structural parameters such as crystallite size, percent crystallinity, strains, stress, and crystal defects. It is commonly used characterization technique for almost all real-world materials as it can provide valuable information for their degree of crystallinity. The prepared sample were subjected to XRD analysis to detect the crystalline phase, orientation, atomic arrangements and particle size. The data obtained from X-ray studies were plotted in the form of graph with the help of origin pro 2019 software. The peaks were analyzed and their 2θ values were noted and analyzed to indexing the peaks [4].

The green synthesized tin oxide nanoparticles employing *P. guajava* leaf extract was demonstrated and confirmed by the characteristic's peaks observed in the XRD image which was illustrated in the **Fig. 1** given below. The XRD pattern shows three intense peaks in the whole spectrum of 2θ value ranging from 20 to 55. A number of Bragg's reflection peaks with 2θ values are 26.71, 34.01, 38.08, 51.90, 54.89, 57.94, 62.03, 64.92, 66.10, 71.41, 78.85 and 83.90 which are related to planes having miller indices (110), (101), (200), (211), (220), (002), (310), (112), (301), (202), (321) and (222) respectively corresponds to tetragonal rutile structure of SnO_2 nanoparticles [10,11] and compared with the standard powder diffraction card of the Joint Committee on Powder Diffraction Standards (JCPDS File No. 41-1445). Thus, the formation of tetragonal-structured SnO_2 was confirmed. The crystallite size of as-prepared SnO_2 nanoparticles was found to be 26.7 nm corresponding to (101) plane which was calculated by using Debye-Scherer equation. It was found that the average size from XRD data was approximately 19.5 nm which illustrate cheat that SnO_2 NPs synthesized by using *P. guajava* leaf extract were

nanocrystalline in nature [10].

The peak broadening in XRD basically depends upon two factors i.e., lattice strain and crystallite size, which are obtained from Williamson-Hall plot. 4εtanθ gives the strain broadening and kλ/Dcosθ gives the broadening due to small crystallite size. βcosθ was plotted against 4sinθ, where the slope and y-intercept of the fitted line represent the strain and the size of the nanoparticles respectively. From the intercept of the Williamson-Hall plot **Fig. 1(B)**, the average particle size was found to be 21.59 nm. **Fig. 1(C)**, given below is the Lorentzian fitting of XRD pattern of SnO_2 NPs synthesized by using *P. guajava* leaf extract done to determine the average particle size. The average particle size was found to be 19.5 nm.
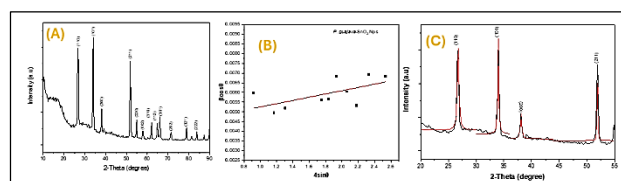
Fig. 1. SnO_2 NPs synthesized by using *P. guajava* leaf extract (**A**) XRD pattern, (**B**) Williamson Hall plot, (**C**) Lorentzian fitting

FTIR Analysis

FTIR measurement was carried out to investigate the functional group associated to tin oxide nanoparticles synthesized using *P. guajava* and extract, as a reducing and capping agent. The FTIR spectrum of SnO_2 NPs (**Fig. 2**) have the bands at 3930 cm^{-1}, 3760 cm^{-1}, 3400 cm^{-1}, 2900 cm^{-1}, 2450 cm^{-1}, 2350 cm^{-1}, 2150 cm^{-1}, 1650 cm^{-1}, 1400 cm^{-1}, 1075 cm^{-1}, 705 cm^{-1} and 450 cm^{-1}. The broad absorption band at 3400 cm^{-1} corresponds to the stretching vibration of O-H group raised due to the presence of adsorbed water molecules on the sample surface. The peak at 2900 cm^{-1} and 1400 cm^{-1} which indicates the presence of alkyl group, are due to asymmetric and symmetric of C-H stretching present in the guava extract. The

peak observed at 2350 cm^{-1} is assigned to the existence of CO_2 molecules in air. The peak at 2150 cm^{-1} indicates the presence of alkynes group. The peak at 1650 cm^{-1} indicates the stretching of amide (C=O) group. The set of peaks in the range of 1400-1075 cm^{-1} is due to the vibration of hydroxyl tin bonds. Similarly, the strong peak between 705 cm^{-1} and 450 cm^{-1} are attributed to the anti-symmetric Sn-O-Sn stretching of the oxide bridge functional group which confirms the formation of SnO_2 NPs [12].
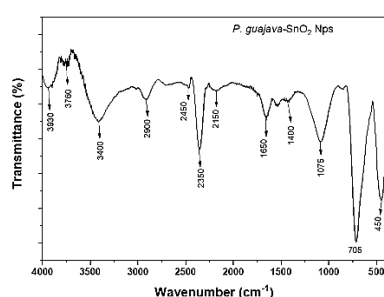
Fig. 2. FTIR spectra of SnO_2 NPs.

UV-Visible analysis

The formation of tin oxide nanoparticles was assessed by using UV-visible spectrophotometer. In case of SnO_2 nanoparticles synthesized using *P. guajava* leaf extract, it was observed that optical absorbance spectra or surface plasmon peak occurred at 270 nm which is due to the presence of various ingredients in the guava leaves which results in the formation of tin ions as shown in the **Fig. 3(A)**. A broad and sharp absorption peak was observed in the spectrum at 270 nm, which is the characteristic band for the pure SnO_2 NPs. Absence of any other peak confirms that the synthesized products was SnO_2 NPs. The obvious red shift in the absorption edge was observed for SnO_2 NPs. This might be due to the changes in their morphologies, particle size, surface microstructure and temperature. There is little sharp increase in absorption peak at 270 nm in the ultraviolet region and it started to decrease linearly up to visible region [18].
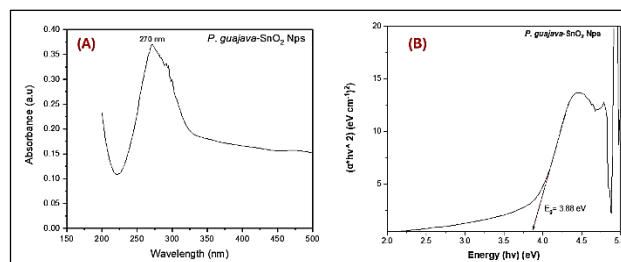
Fig. 3. (**A**) UV-Visible spectra of SnO_2 NPs, (**B**) Plot of Photon energy (hν) versus (αhν)^2 of SnO_2 NPs.

The UV-Visible absorption ability of nanoparticles is related with the band gap energy of the particle. The UV-visible absorption edge provides a reliable estimate of band gap of any system. **Fig. 3(B)** displays the Tauc plot where (αhν)^2 is plated as a function of hν for tin oxide nanoparticles. The linear portion of the curve is extrapolated to (αhν)^2 = 0, from where direct band gap of the SnO_2 NPs was extracted. The band gap energy of the tin oxide nanoparticles was calculated based on formulae as given below [19].

$$E_g = 1240/\lambda \ (eV) \tag{2}$$

Where, λ is the wavelength of the sample and hν is calculated by using following formulae.

$$h\nu = 1240/wavelength \ (nm) \tag{3}$$

Where, hν = Incident photon energy

The band gap is calculated by extrapolating the curve drawn (hν) versus (αhν)^2 to the X-axis as shown in the **Fig. 3(B)** above. By this procedure the band gap energy was calculated 3.88 eV for *P. guajava* tin oxide nanoparticles which is shown in the **Fig. 3(B)** given above [24].

Antioxidant activity (DPPH assay)

Antioxidant activity of prepared tin oxide nanoparticles was determined by using DPPH assay method. The DPPH radical absorbs at 517 nm and antioxidant activity can be determined by monitoring the decrease in the absorbance. All statistical analysis is performed using Origin pro 2019 software. The obtained data are tabulated below [28,29]. Absorbance of control = 1.102 nm

137

Inhibition percentage (%) = absorbance of control – absorbance of sample × 100/

Absorbance of control

Table 1: Determination of antioxidant property of tin oxide nanoparticles synthesized using *P. guajava* leaf extract.

Concentration of sample (mg/mL)	Absorbance of sample (nm)	Inhibition percentage (%)
10	1.0102	8.33
20	0.9866	10.47
30	0.9331	15.32
40	0.8686	21.17
50	0.7074	35.80

Estimation of free radical scavenging activity using 2,2-diphenyl-1-picryl hydrazyl (DPPH) is commonly used to evaluate the antioxidant potential of nanoparticles. DPPH, a deep purple color stable free radical turns into light yellow color when scavenged or reduced. When the SnO_2 Nps are mixed into DPPH solution, the solution will slowly change from deep purple or violet color to light yellow color, demonstrating the scavenging potential or antioxidant activity of SnO_2 Nps [28].
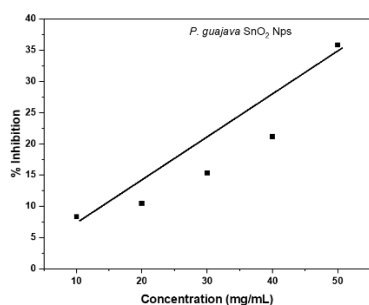
Fig. 4. Graphical representation of inhibition % versus concentration (mg/mL) of antioxidant activity of SnO_2 NPs synthesized using *P. guajava* leaf extract.

The odd electron or the free radical of the DPPH pair with a cation from antioxidant compounds present in guava leaves, thus reducing or scavenging the DPPH to form DPPH-H.

Maximum inhibition percentage of SnO_2 NPs was found at concentration 50 mm The

histogram shows that SnO_2 NPs possess good antioxidant property. The effect of activity depends on the site of attachment of the metal, particle size, morphology, defects and other variables.
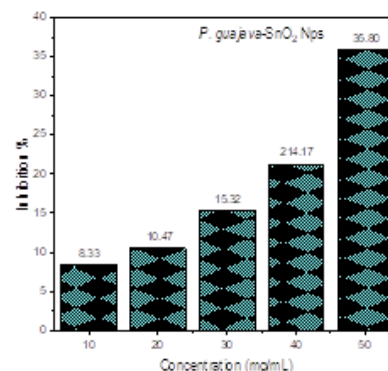
Fig. 5. Antioxidant activity of SnO_2 NPs against DPPH using *P. guajava* leaf extract.

The percentage of free radical scavenging activity at different concentration ranging from 10 to 50 mg/mL for the tin oxide nanoparticles was evaluated. It was found that antioxidant activity varied with concentration.

Antibacterial activity

The antibacterial activity of the tin oxide nanoparticles was established by disc diffusion method and their potency was determined by measuring the diameter of zone of inhibition (ZOIs). The antibacterial activity of sample of tin oxide nanoparticles were observed in two Gram-negative bacteria *Klebseilla pneumoniae* ATCC 700603, *Pseudomonas aeruginosa* ATCC 27853 *and* one Gram-positive bacteria *Staphylococcus aureus* ATCC 6538P as shown in **Fig. 6(A), 6(B)** and **6(C)**, respectively. Inhibitory zone in agar plate was seen which indicates the presence of antibacterial activity of tin oxide nanoparticles [30-32]. Some representative pictures of tin oxide nanoparticles which showed the zone of inhibition (ZOIs) against different microorganisms were presented in figure 6 below.
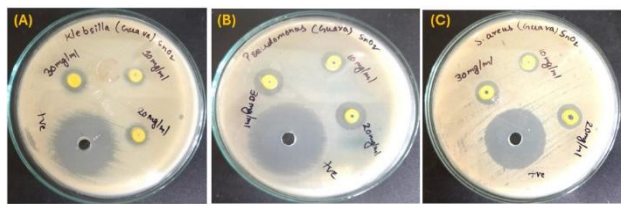
Fig. 6. Photographs showing antibacterial tests of tin oxide NPs against (**A**) *P. aeruginosa* (**B**) *K. pneumoniae* (**C**) *S. aureus.*

Here, we can see that the SnO_2 NPs showed greater activity against Gram-negative bacteria instead of Gram-positive bacteria. This is ascribed to the differentiation in chemical structure of the cell wall of both bacteria. The thick peptidoglycan layer present in the cell wall of Gram-positive bacteria provides more strength and shows greater resistance whereas the cell wall of Gram-negative bacteria is made of up soft layer of peptidoglycan, which facilitate the entry of penetrating agent.

Table 2. Comparison of antibacterial activity of SnO_2 NPs with standard antibiotics kanamycin [26].

Pathogens	Concentration of samples (mg/mL)	Diameter of zone of inhibition (mm)	Standard kanamycin (5µg/disc)
S. aureus	10	7	
	20	12	23
	30	18	
P. aeruginosa	10	10	
	20	13	24
	30	21	
K. pneumonia	10	8	
	20	10	23
	30	20	

Conclusions

SnO_2 NPs were synthesized successfully by co-precipitation green synthetic route at ambient condition. The average particle size as calculated by using Debye-Scherer's equations was found to be 19.5 nm. In addition, the average particle size calculated by using Williamson-Hall plot method was found to be 21.59 nm. The lattice strain(ε) of as-synthesized SnO_2 NPs was found to be 8.38×10^{-4}. The dislocation density (δ) of as-synthesized SnO_2 NPs was found to be 2.45 (nm^{-2}). The FTIR

spectra reveals hydroxyl, alkyl, alkane, amide and hydroxyl tin group as a functional group. UV-Visible absorption spectra were found to be 270 nm, and its corresponding band gap energy was found to be 3.88 eV. The antibacterial activity against different bacteria shows the clear zone of inhibitions due to the presence of medicinally active phyto-chemicals constituents present in *P. gaujava* leaf extract. The antibacterial activity of SnO_2 NPs was found to be more effective towards Gram-negative bacteria than in Gram-positive bacteria. The antioxidant activities of tin oxide nanoparticles increase with increase in concentration of nanoparticles. Since the synthesized SnO_2 NPs are ecofriendly and biocompatible, these SnO_2 NPs have the potential to offer their application in biomedical and related fields to improve the quality of life.

Author's Contribution Statement

Tirtha Raj Binadi: Methodology, Writing: original manuscript, review and editing, Data curation, **Paramatma Mishra:** Methodology, and Writing: orinial manuscript, review and editing, **Bhoj Raj Poudel:** Data analysis, Writing: review and editing, **Surendra K. Gautam:** Conceptualization, Supervision, Data analysis, and Writing: review and editing

Conflict of Interest

The authors do not have any conflict of interest throughout this research work.

Data Availability Statement

The data supporting this study's findings are available from the corresponding authors upon

reasonable request.

References

1. B. E. Ghmari, H. Farah and A. E. Chahad, Biosynthesis, characterization of nickel(ii) oxide nanoparticles NiO and their efficient photocatalytic application, *International Journal of Nanoscience and Nanotechnology.*, 2023, 19(3), 135-147. DOI: 10.22034/ijnn.2023.560608.2262

2. S. Dhungana, B. R. Paudel, and S. K. Gautam, Synthesis and characterization of ZnTe nanoparticles, *Nepal Journal of Science and Technology*, 2016, 17(1), 1–3. (DOI: 10.3126/njst. v17i1.25054)

3. B. B. Neupane, B. Pandey, B. Giri and M. K. Joshi, A textbook of nanoscience and nanotechnology, publidhed by Heritage publishers and distributers Pvt. Ltd., 2016, ISBN:978-9937-595-87-2.

4. S. Dhungana, A. Gauli, L. Tiwari, D. Khadka, S. K. Gautam, M. R. Pokhrel, J. Baral and B. R. Poudel, Synthesis and Characterization of Copper Oxide Nanoparticles Isolated from *Acmella oleracea* and Study of Antimicrobial and Phytochemical Properties, *Amrit Research Journal*, 2023, 5(1), 18-29. https://doi.org/10.3126/arj.v5i1.73521

5. A.G. Habte, F.G. Hone and F.B. Dejene, Influence of Cu- Doping concentration on the structural and optical properties of SnO_2 nanopartices by co-precipitation route, *Journal of Nanomaterials.*, 2022, 1-10. Doi: 10.1155/2022/5957125

6. S. Tazikeh, A. Akbari, A. Tabeli and E. Tabeli, Synthesis and characterization of tin oxide nanoparticles via the Co-precipitation method, *Materials Science-Poland.*, 2014, 32(1), 98-101. DOI: 10.2478/s13536-013-0164-y

7. J.Singh, T. Dutta, K.H. Kim, M. Rawat, P. Sanddar and P. Kumar, Green synthesis of metal and their oxide nanoparticles: applications for environmental remediation, *Journal of Nanobiotechnology.*, 2018, 16(84), 1-14. DOI: 10.1186/s12951-018-0408-4

8. S. Gorai, Bio-based synthesis and application of tin oxide nanoparticles – an overview, *Journal of Materials and Environmental Science.*, 2018, 9(10), 2894-2903.

9. Y. T. Gebreslassie and H. G. Gebretnsae, Green and cost effective synthesis of tin oxide nanoparticles, a review on the synthesis methodologies, mechanism of formation and their potential applications, *Nanoscale Research Letters.*, 2021, 16(97), 1-16. DOI: 10.1186/s11671-021-03555-6

10. M. Kumar, A. Mehta, A. Mishra, J. Singh, M. Rawat and S. Basu, Biosynthesis of tin oxide nanoparticles using Psidium guajava leave extract for photocatalytic dye degradation under sunlight, *Materials Letters.*, 2018, 215, 121-124. DOI: 10.1016/j.matlat.2017.12.074

11. S. Sagadevan, J. A. Lett, I. Fatimah, Y. Lokanthan, E. Leonard, W. C. Oh, M. A. M. Hossai and M. R. Johan, Current trends in the green synthesis of tin oxide nanoparticles and their biomedical applications, *Materials Research Express.*, 2021, 8, 1-14. DOI: 10.1088/2053-1591/ac187e

12. P. A. Luque, M. J. C. Chinchillas, O. Nava, E. L. Medina, M. E. M. Rosas, A. C. Costillo, A. R. V. Nestor, L. E. M. Munoz and H. E. G. Galvez, Green synthesis of tin oxide nanoparticles using Camellia sinensis and its applications in photocatalytic degradation of textile dyes, *International Journal for Light and Electron Optics.*, 2021, 229, 1-4. DOI: 10.1016/j.ijleo.2021.166259

13. S. P. Patil and P. M. Rane, Psidium guajava leaves assisted green synthesis of metallic nanoparticles: a review, *Beni Suef University Journal of Basic and Applied Science.*, 2020, 9(60), 1-7. DOI: 10.1186/s43088-020-00088-2

14. W. Ahmad, A. Pandey, V. Rajput, V. Kumar, M. Verma and H. Kim, Plant extract mediated cost-effective tin oxide nanoparticles: A review on synthesis, properties, and potential applications, *Current Research in Green and Sustainable Chemistry.*, 2021, 4, 1-11. DOI: 10.1016/j.crgsc.2021.100211

15. P. S. S. Selvam, D. Ganesan, V. Rajangam, A.

Raji and V. Kandan, Green synthesis of SnO₂ nanoparticles for catalytic degradation of rhodamine B*, Iranian Journal of Science and Technology, Transaction Science.*, 2020, 1-16. DOI: /10.1007/s40995-020-00885-5

16. I. Buniyamin, N. A. Asli, M. H. F. Suhaimi, K. A. Eswar, M. Mohammad, M. R. Mahmood and Z. Khusaimi, The photocatalytic characteristics of tin oxide nanoparticles synthesized through Aquilaria malaccensis, *International Journal of Chemical and Biochemical Sciences.*, 2023, 24(7), 63-73.

17. N. Awoke, D. Pandey and A. B. Habtemariam, Synthesis of tin(IV) oxide nanoparticles using plant leaf extracts of Vernonia amygdalina and Mentha spicata, *Regenerative Engineering and Translational Medicine.*, 2021, 1-6. https://doi.org/10.1007/s40883-021-00218-x

18. K. C. Suresh, S. Surendhiran, P. M. Kumar, E. R. Kumar, Y. A. S. Khadar and A. Balamurugan, Green synthesis of SnO₂ nanoparticles using Delonix elata leaf extract: Evaluation of its structural, optical, morphological and photocatalytic properties, *SN Applied Science*, 2020, 2(1735), 1-13. | https://doi.org/10.1007/s42452-020-03534-z

19. S. Matussin, M. H. Harunsani, A. L. Tan and M. M. Khan, Plant extract-mediated SnO₂ nanoparticles: Synthesis and applications, *ACS Sustainable Chemistry & Engineering.*, 2020, 1-49. DOI: 10.1021/acssuschemeng.9b06398

20. N. Aggarwal, H. Kaur, N. Kumar, J. Kaur, S. Malhotra, A. Sharma, S. Tripathi, R. S. Panwar and P. Patial, Evaluation of photocatalytic efficacy of biosynthesized tetragonal SnO₂ nanoparticles, *Results in Chemistry.*, 2023, 5, 1-4. Doi: 10.1016/j.rechem.2023.100803

21. A. Regmi, Y. Basnet, S. Bhattarai and S. K. Gautam, Cadmium sulfide nanoparticles: Synthesis, Characterization, and antimicrobial study, *Journal of Nanomaterials.*, 2023, 1-7. Doi:10.1155/2023/8187000

22. U. Riaz and J. Zia, Microwave-assisted rapid degradation of DDT using nanohybrids of 2 PANI with SnO₂ derived from Psidium guajava extract*,

Environmental Pollution (2020), 1-34. https://doi.org/10.1016/j.envpol.2020.113917

23. G. Elango, S. M. Kumaran, S. S. Kumar, S. Muthuraja and S. M. Roopan, Green synthesis of SnO₂ nanoparticles and its photocatalytic activity of phenolsulfonphthalein dye, *Spectrochimica Acta Part A: Molecular and Biomolecular Spectroscopy.*, 2015, 145, 176-180. http://dx.doi.org/10.1016/j.saa.2015.03.033

24. S. K. Gautam, B. Sapkota, A. Bhujel and S. Bhattarai, Estimation of particle size and band gap of zinc oxide nanoparticles synthesized by chemical precipitation method, *Journal of Nepal Chemical Society.*, 2020, 41(1), 46-50. DOI: 10.3126/jncs. v41i130448

25. N. A. I. M. Ishak, S. K. Kamarudin and S. N. Timmiati, Green synthesis of metal and metal oxide nanoparticles via plant extracts: an overview, *Materials Research Express.*, 2019, 6, 1-32. DOI 10.1088/2053-1591/ab4458

26. A. Diallo, E. Manikandan, V. Rajendran and M. Maaza, Physical & enhanced photocatalytic properties of green synthesized SnO₂ nanoparticles via Aspalathus linearis, *Journal of Alloys and Compounds.*, 2016, 681, 561-570. http://dx.doi.org/10.1016/j.jallcom.2016.04.200

27. S. Z. Ajabshira, M. S. Morassaeib , O. Amiric and M. S. Niasari, Green synthesis of dysprosium stannate nanoparticles using Ficus carica extract as photocatalyst for the degradation of organic pollutants under visible irradiation, *Ceramics International.*, 2019, 1-13. https://doi.org/10.1016/j.ceramint.2019.11.072

28. V.K. Vidhu and D. Philip, Biogenic synthesis of SnO₂ nanoparticles: Evaluation of antibacterial and antioxidant activities, *Spectrochimica Acta Part A: Molecular and Biomolecular Spectroscopy.*, 2015, 134, 372-379. http://dx.doi.org/10.1016/j.saa.2014.06.131

29. P. Sharma, S. Dhungana, R. Rai, D. Khadka, D. K. Hitan, M. R. Pokhrel, S. K. Gautam and Bhoj Raj Poudel, Temperature dependent synthesis of zinc sulphide nanoparticles and its

characterization, *Amrit Research Journal.*, 2022, 3(1), 67-74.

30. A. Bhujel, B. Sapkota, R. L. Aryal, B. R. Poudel, S. Bhattarai and S. K. Gautam, Insight of precursor concentration, particle size and band gap of zirconia nanoparticles synthesis by co-precipitation method, *Bibechana.*, 2021, 18(1), 1-9. Doi: 10.3126/bibechana.v18i1.28958

31. S. Abirami , G. Viruthagiri and K. Ashokkumar, Structural, morphological and anti - bacterial activities of pure SnO_2 nanoparticles prepared by chemical precipitation method, *Materialstoday:Proceedings.*, 73(3), 2023, 535-538. Doi: 10.1016/j.matpr.2022.11.442

32. D. Khadka, P. Gautam, R. Dahal, M. D. Ashie, H. Paudyal, K. N. Ghimire, B. R. Poudel, M. R. Pokhrel, Evaluating the Photocatalytic Activity of Green Synthesized Iron Oxide Nanoparticles, *Catalysts*, 2024, 14(11), 751. https://doi.org/10.3390/catal14110751